Matrix Biology 33 (2014) 68–76

Contents lists available at ScienceDirect

Matrix Biology

journal homepage: www.elsevier.com/locate/matbio

Influence of biological matrix and artificial electrospun scaffolds on proliferation, differentiation and trophic factor synthesis of rat embryonic stem cells

M. Alessandri [a,1], G. Lizzo [b,1], C. Gualandi [c,d], C. Mangano [b], A. Giuliani [b], M.L. Focarete [a,c,*,2], L. Calzà [a,b,**,2]

[a] Health Sciences and Technologies-Interdepartmental Center for Industrial Research (HST-ICIR), University of Bologna, Bologna, Italy
[b] Department of Veterinary Medical Science, University of Bologna, Bologna, Italy
[c] Department of Chemistry "G. Ciamician" and National Consortium of Materials Science and Technology (INSTM, Bologna RU), University of Bologna, Bologna, Italy
[d] Advanced Applications in Mechanical Engineering and Materials Technology. Interdepartmental Center for Industrial Research, University of Bologna, Bologna, Italy

ARTICLE INFO

Article history:
Received 23 May 2013
Received in revised form 2 August 2013
Accepted 2 August 2013

Keywords:
Embryonic stem cell
Poly(lactic acid)
Extracellular matrix
Scaffold
Electrospinning
Growth factors

ABSTRACT

Two-dimensional *vs* three-dimensional culture conditions, such as the presence of extracellular matrix components, could deeply influence the cell fate and properties. In this paper we investigated proliferation, differentiation, survival, apoptosis, growth and neurotrophic factor synthesis of rat embryonic stem cells (RESCs) cultured in 2D and 3D conditions generated using Cultrex® Basement Membrane Extract (BME) and in poly-(L-lactic acid) (PLLA) electrospun sub-micrometric fibres. It is demonstrated that, in the absence of other instructive stimuli, growth, differentiation and paracrine activity of RESCs are directly affected by the different microenvironment provided by the scaffold. In particular, RESCs grown on an electrospun PLLA scaffolds coated or not with BME have a higher proliferation rate, higher production of bioactive nerve growth factor (NGF) and vascular endothelial growth factor (VEGF) compared to standard 2D conditions, lasting for at least 2 weeks. Due to the high mechanical flexibility of PLLA electrospun scaffolds, the PLLA/stem cell culture system offers an interesting potential for implantable neural repair devices.

1. Introduction

The influence of tridimensional (3D) microenvironment ("niche") in stem cells biology is well known and established (Brizzi et al., 2012; Zapata et al., 2012). The chemical composition of the extracellular matrix (ECM), free- and ECM-linked bioactive molecules, and mechanic and adhesive forces generated in this dynamic space are key players in stem cell proliferation, differentiation and migration (Blancas et al., 2011; Pineda et al., 2013). In spite of this, 3D *in vitro* systems considering ECM properties are still poorly used for stem cell biology studies, as compared to conventional 2D culture systems. This is even more surprising when *in vitro* studies are directed to understand the possible use of stem cells for regenerative medicine purposes.

Tissue engineering technologies and material science are offering a wide range of possibilities for tailoring mechanical and chemical properties of new scaffolds to host stem cells according to specific purposes, *i.e.* "*in vitro*" niche reproduction, stem cell properties regulation, transplant of scaffold/cell mixed devices, *etc.* (Dickinson et al., 2011; Edalat et al., 2012).

In this study we investigated properties of rat embryonic stem cells (RESCs) (Fernandez et al., 2011) cultured in different 2D and 3D systems, conjugated or not to ECM components, focusing on the synthesis of growth and trophic factors of interest for neural repair. To create 3D systems, we used Basement Membrane Extract (BME) as "natural" microenvironment and poly(L-lactic acid) (PLLA) electrospun sub-micrometric fibers as artificial scaffold possibly usable for *in vivo* application. Cultrex® BME is a soluble form of basement membrane purified from Engelbreth–Holm–Swarm (EHS) tumor, including laminin, collagen IV, entactin, and heparin sulfate proteoglycan. PLLA fibrous scaffolds were fabricated by electrospinning. The properties of RESCs grown on these 3D systems were compared to standard conditions (2D culturing on either glass or plastic) with regard to proliferation, differentiation, survival, apoptosis and paracrine properties useful for neural repair.

* Correspondence to: M.L. Focarete, Department of Chemistry 'G. Ciamician', University of Bologna, Via Selmi 2, 40126 Bologna, Italy. Tel.: +39 051 209 9572; fax: +39 051 209 9456.
** Correspondence to: L. Calzà, Health Sciences and Technologies-Interdepartmental Center for Industrial Research (HST-ICIR), University of Bologna, Via Tolara di Sopra 41/E, I-40064 Ozzano Emilia Bologna, Italy. Tel.: +39 051 798776; fax: +39 051 799673.
E-mail addresses: marco.alessandri2@unibo.it (M. Alessandri), giulia.lizzo@yahoo.it (G. Lizzo), c.gualandi@unibo.it (C. Gualandi), a.giuliani@unibo.it (A. Giuliani), marialetizia.focarete@unibo.it (M.L. Focarete), laura.calza@unibo.it (L. Calzà).
[1] These authors contributed equally to the study.
[2] These authors share senior authorship.

0945-053X/$ – see front matter © 2013 Elsevier B.V. All rights reserved.
http://dx.doi.org/10.1016/j.matbio.2013.08.001

2. Results

The following culture conditions were used and compared in the study: (i) es-PLLA fibrous scaffolds (3D); (ii) es-PLLA fibrous scaffolds coated with BME (3D); (iii) 3D-BME (3D); (iv) plastic/glass (2D); and (v) plastic/glass coated with BME (2D). For growth factor expression analysis, also embryonic bodies (EB) derived from RESCs have been included. RESC growth, early differentiation and paracrine properties were assessed in short (3 DIV) and long (15 DIV) culture conditions.

2.1. Proliferation, survival, stemness and differentiation of RESCs in different 2D and 3D culture conditions

In the first part of the study the effect of culturing conditions on the main biological characteristics of RESCs, such as viability and proliferation, general morphology and the expression of pluripotency markers, were investigated.

The MTT viability assay was used to study cell viability and proliferation at different days in culture (up-to 5 DIV). Since the cell death, as investigated by nuclear morphology and caspase expression, is similar in the different conditions (except for 3D-BME), the MTT results can reasonably reflect cell proliferation. Results are reported in Fig. 2A. In a 5-day cell culture, BME coated PLLA and es-PLLA scaffolds promoted an increase in RESC growth compared to plastic (Fig. 2A). The comparative analysis of pyknotic nuclei in all culture conditions performed at 3, 6 and 12 DIV indicated a significant increase in nuclear condensation and fragmentation in 3D-BME at 6 DIV and a 10-fold increase at 12 DIV *vs* glass (similar to plastic, *data not shown*) (Fig. 2B). Panel 2C illustrates pyknotic (head of arrow) and fragmented (thin arrows) nuclei after Hoechst 33342 staining. According to this, a high percentage of active-caspase-3 positive cells was counted in long-term 3D culture (Fig. 2D). Panel 2E illustrates a caspase 3-pyknotic nucleus (arrow).

The spontaneous aggregation and culture attitude of the RESCs grown on different substrates was then analyzed using actin immunostaining. When seeded on plastic, glass or BME coated plastic/glass, cells were arranged in a monolayer of either round or spindle-shaped cells (Fig. 2G). A 3D-BME environment promoted the growth of spheric-like structures; after a few days culture, the spheres developed empty central cavities resembling embryoid bodies (Fig. 2F). On es-PLLA scaffolds, closely connected round-shaped cells grew forming a ring-like structure with a diameter ranging from 20 to 40 μm (Fig. 2H). The es-PLLA scaffold was characterized by a rather narrow fibrous mesh, so that the cells remained spread over the surface, without infiltrating deep into the fiber network (Fig. 1B, C).

In order to assess whether culturing conditions affects RESCs stemness, the expression of octamer-binding transcription factor 4 (Oct4), a marker associated with pluripotency (Li et al., 2010; Fernandez et al., 2011; Ou et al., 2011), was investigated at 15 DIV in the different culture conditions. Results are presented in Fig. 3. While 2D-culture did not change the Oct4 mRNA expression in long-term culture, 3D long-term grown culture in 3D-BME increased Oct4 expression level, thus supporting the stemness properties of these cells. Conversely, the long-term grown on either uncoated or BME-coated es-PLLA reduced the Oct4 expression level, thus suggesting a pro-differentiative action. Oct4 protein was expressed in all cells when visualized by immunocytochemistry (Fig. 3B–E).

The expression of nestin and alpha-fetoprotein (AFP), which are lineage-associated markers, was then analyzed and the results are illustrated in Fig. 4. Nestin showed a cytoplasmic or peri-nuclear distribution, while AFP displayed a dotted cytoplasmic localization in all investigated conditions. In glass and BME-glass (Fig. 4A, B) almost all cells were Nestin-positive, while in es-PLLA and 3D-BME (Fig. 4C, D) few cells were Nestin-negative. Eventhought AFP immunoreactivity was homogeneously distributed within cell population in all the investigated conditions, few differences in the staining intensity could be appreciated only in RESCs cultured on es-PLLA, especially in the internal side of the ring. When cultured in 3D conditions, either es-PLLA or 3D-BME, RESCs spontaneously aggregated to form follicle-like structures, thus suggesting the 3D microenvironment favors shaping multicellular aggregates.

2.2. Paracrine properties

An important issue in regenerative medicine is the role of growth factors in neuroprotection and damage repair. In order to assess how the culture conditions influence the paracrine properties of RESCs, the production of growth (VEGF) and neurotrophic factors (NGF, BDNF) was investigated by semiquantitative real-time PCR at 3, 7 and 15 DIV (days *in vitro*). The growth factor expression profile is shown in Fig. 5, using 3 DIV plastic as the reference mRNA level. The statistical analysis was performed using two-ways ANOVA to analyze both time and culture condition effects; at each time point, one-way ANOVA and post-hoc test *vs* the respective control (plastic) culture condition were also performed and presented in Fig. 5.

A time-dependent, 10- to 30-fold increase in the VEGF mRNA levels occurred in all the culture conditions (Fig. 5A). Notably, manipulation of

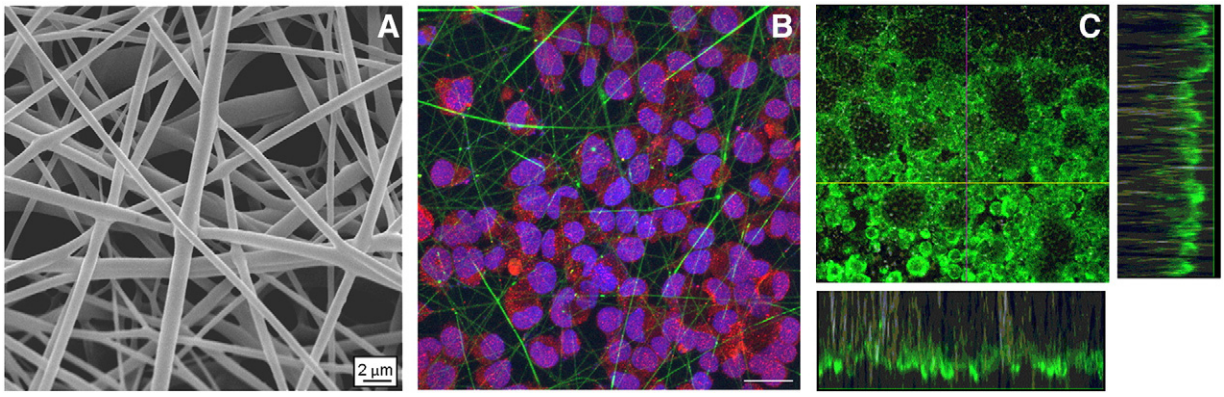

Fig. 1. es-PLLA scaffold and RESCs on scaffold. A: SEM micrograph of PLLA electrospun scaffold; Scale bar: 2μm. B: Representative picture of RESC cells grown on es-PLLA scaffold; B: cells were visualized by actin staining (red) and nuclear Hoechst33258 staining (blue); es-PLLA fibers were labeled with FITC (green); *Scale bar:* 20 μm. C: 3D visualization of RESCs by Oct4 immunostaining (green) in confocal microscopy; Purple and yellow lines represent *xy* visualization of *yz* and *xz* orthogonal planes, respectively. Side and bottom panels represent purple line *yz* projection and yellow line *xz* projection, respectively; cells grew as a monolayer on es-PLLA scaffold and are localized on the scaffold surface.

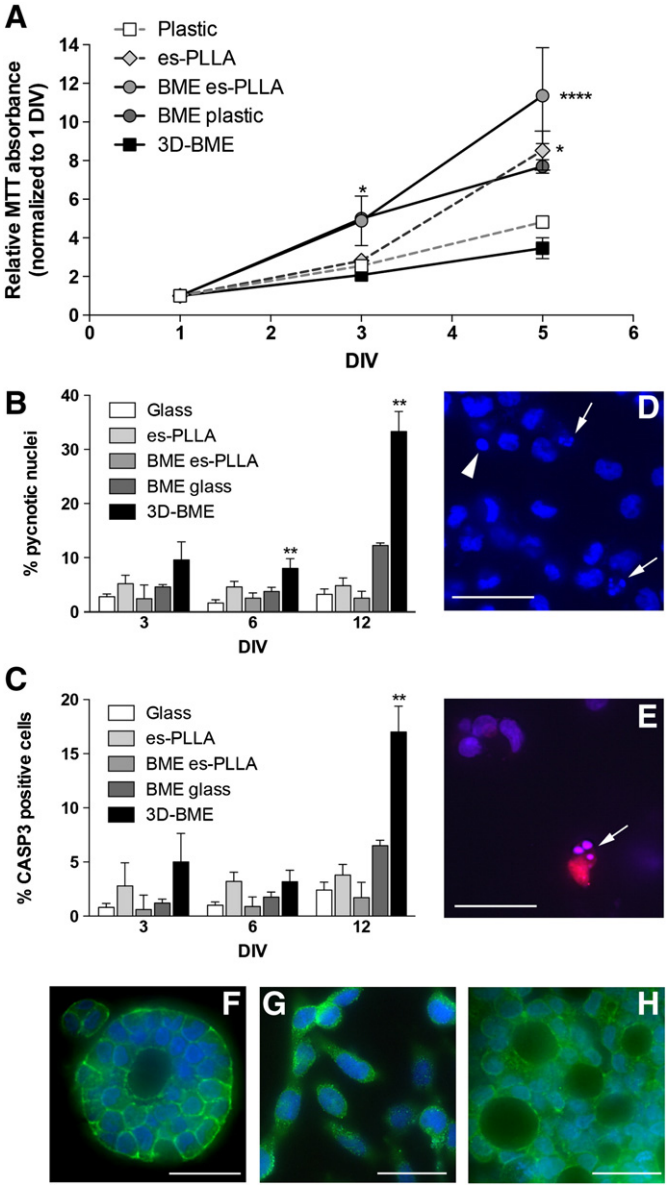

Fig. 2. Proliferation and viability assays of RESCs cultured on different 2D and 3D surfaces. A: the graph shows the relative MTT absorbance at 1, 3 and 5 DIV, normalized to 1 DIV for each surface (plastic, es-PLLA scaffolds, BME-coated es-PLLA, BME-coated plastic and 3D-BME); B: percentage of pyknotic nuclei visualized by Hoechst33258 staining at 3, 6 and 12 DIV; C: Percentage of Caspase3 immunoreactive cells on total cell number; D: representative picture of Hoechst33258 staining and evidence of pyknotic (blue, arrow head) and fragmented nuclei (blue, arrow). E: Hoechst33258 and Caspase3 staining (red, arrow). F–H: Representative picture of cell growth visualized by actin immunostaining (green) in 3D-BME (F), glass (G), and es-PLLA scaffold (H). *Statistical analysis:* In A all data sets were analyzed by two-way ANOVA followed by Bonferroni post test, considering "plastic" as control group. In B and D each data set corresponding to 3, 6, 12 DIV was analyzed by one-way ANOVA followed by Dunnet's post test, with "glass" as the control group. * $p < 0.05$, ** $p < 0.01$, **** $p < 0.0001$. *Scale bar:* 20 μm.

culturing conditions either in 3D (es-PLLA, BME es-PLLA and 3D-BME) and in 2D (BME plastic) further increase VEGF mRNA expression at 15 DIV compared to standard 2D culturing (plastic) (two-ways ANOVA: culture condition effect: ***$p < 0.0001$, $F(5,36) = 15.68$, time effect: ***$p < 0.0001$, $F(2,36) = 451.81$, interaction: ***$p < 0.0001$, $F(10,36) = 10.17$).

NGF mRNA expression level was differentially affected by the culturing conditions at short (3 DIV) and long (15 DIV) time (culture condition effect: ***$p < 0.0001$, $F(5,35) = 42.41$, time effect: ***$p < 0.0001$, $F(2,35) = 123.51$, interaction: ***$p < 0.0001$, $F(10,35) = 29.41$). At short time, 3D culture in "natural" microenvironment (*i.e.* 3D-BME and EB) strongly up-regulated NGF mRNA expression level, which was down-regulated in long-term culture. On the contrary, the growth on artificial 3D microenvironment created by PLLA, either coated or not with BME, strongly up-regulated NGF mRNA expression level in long-term culture.

BDNF mRNA expression level regulation was similar to NGF in "natural" *vs* artificial microenvironment at short time, while the observed up-regulation was reversed in long-term culture (culture condition effect: ***$p < 0.0001$, $F(5,34) = 19.68$, time effect: ***$p < 0.0001$, $F(2,34) = 29.90$, interaction: ***$p < 0.0001$, $F(10,34) = 7.53$).

Finally, in order to test if the regulation of mRNA expression level reflected the production of biologically active peptide, NGF activity was tested *in vitro* using the classical PC12 neurite elongation test. PC12 neurite outgrowth in the presence of exogenous NGF was compared to culture medium conditioned by RESCs grown on plastic, es-PLLA, BME coated es-PLLA and BME coated plastic (Fig. 6). While control PC12 showed no branching (Fig. 6A), NGF induced differentiation in a higher percentage of cells (Fig. 6B), such as culture medium from RESCs/es-PLLA, RESCs/BME coated es-PLLA and RESCs/BME plastic systems(Fig. 6C). Branching analysis results are reported in Fig. 6D.

3. Discussion

It has been described that *in vivo* microenvironments influence stem cell properties; likewise, many tissue-engineering approaches take advantage of chemical and biological modifications of biomaterials in order to direct cell differentiation and host integration (Gerlach et al., 2010; Li et al., 2010; Ou et al., 2011; Heydarkhan-Hagvall et al., 2012). Cell/scaffold devices applying biochemical stimuli (including soluble and surface-bond signals, cytokines, extracellular matrix components) have been used in niche biomimicking strategies (Johnson et al., 2010; Uemura et al., 2010) or topographic cues, to encourage lineage differentiation (Levenmberg et al., 2003; Xie et al., 2009) or to guide neurite outgrowth and cell migration (Yang et al., 2004). The present study describes different properties of rat embryonic stem cells according to 2D and 3D culture condition obtained by "natural" and "artificial" scaffolds enriched or not of ECM components. We demonstrated that growth, differentiation and paracrine activity of RESCs (synthesis rate of NGF, BDNF, VEGF) are directly affected by the microenvironment, in the absence of other instructive stimuli.

"Natural" 3D microenvironment has been generated by BME preparation. BME is a natural biomaterial enriched with laminin, collagen IV, entactin, heparin sulfate proteoglycan. In 3D-BME, RESC growth was organized in a spheric-like structure with a central cavity, resembling embryoid bodies. During long-term culture, while the spheric-like structure expanded, a marked increase in apoptosis occurred which at least partially contributed to structure re-shaping. The death/proliferation balance was markedly different from the 2D-growth observed over a BME-coated plastic/glass, thus indicating a three-dimensional driven effect. Matrix stiffness might contribute to this balance (Zhang et al., 2011), but no studies have been performed to quantify this effect. Little influence by extracellular matrix (ECM) proteins has been observed in differentiation triggering, since both Oct4 and germ layer specific markers shared a quite similar pattern in 3D-BME, BME-coated plastic and non-coated plastic. Indeed, BME-based biomaterials like Matrigel™ are widely used to facilitate differentiation of ESC or neuronal progenitors but always in the presence of other instructive cues (Levenmberg et al., 2003; Uemura et al., 2010). Chen et al. (2007), by studying the adhesiveness of primate ESC cells to various ECM, described a poor effect of exogenous ECM proteins in triggering differentiation; rather, they showed that ECM encouraged cell–cell interaction and local aggregation, which in turn played a crucial role in controlling gene expression (Chen et al., 2007). The distinct components of BME could also affect RESCs biology. Heparan sulfate (HS) regulates lineage fate (Kraushaar et al., 2013) also toward the

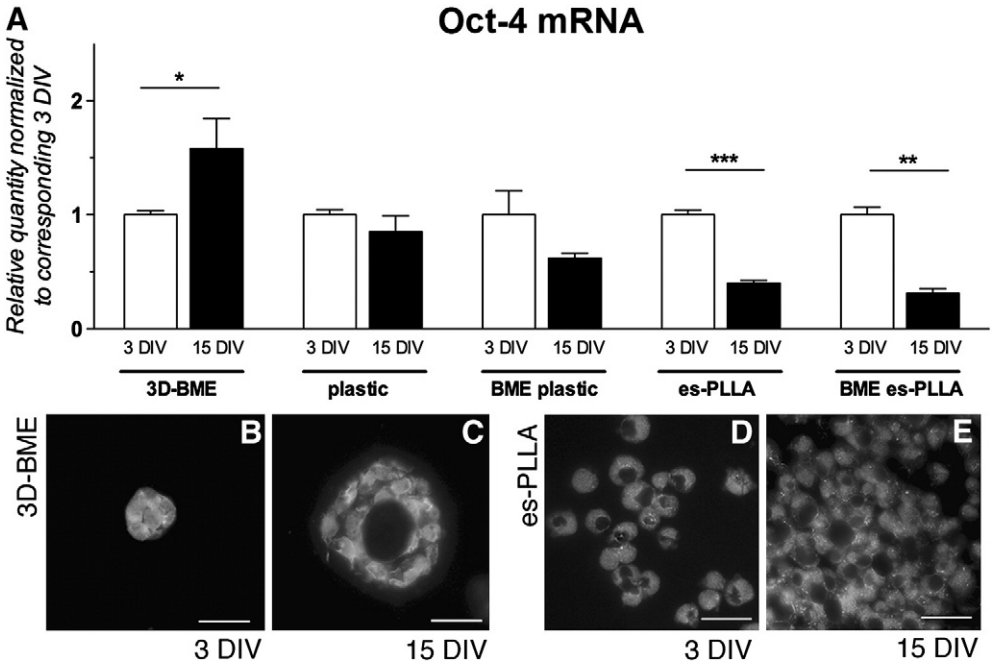

Fig. 3. Oct4 expression in RESCs cultured on different surfaces. A: Real-time PCR analysis of Oct4 mRNA expression in RESCs grown on 3D-BME, plastic, BME-coated plastic, es-PLLA scaffold, BME-coated es-PLLA scaffold at two different time points (3 and 15 DIV). The mRNA expression levels were normalized *vs* the corresponding 3 DIV in each culturing condition. *Statistical analysis:* Students *t* test was used for 3 *vs* 15 DIV comparison in all culturing conditions, $^{*}p < 0.05$, $^{**}p < 0.01$, $^{***}p < 0.001$. B–E: Oct4 immunoreactivity in RESCs cultured on 3D-BME (B, C) and on es-PLLA scaffolds (D, E). *Scale bar:* 20 μm.

neural fate (Johnson et al., 2007) by modulating the functions of numerous growth factors and morphogens, having wide impact on the extracellular information received by cells (Tamm et al., 2012). Laminin favors neurite outgrowth (Dickinson et al., 2011), while collagen IV induces trophoectoderm differentiation of mouse embryonic stem cells (Schenke-Layland et al., 2007).

"Artificial" 3D microenvironment has been generated by electrospun PLLA, a bioresorbable synthetic biomaterial. The use of electrospinning technology allows the fabrication of well-defined micro-nanofibrous structures with controlled shape, thickness and surface properties. The high porosity of the es-PLLA scaffold determines good permeability, which is an important parameter in controlling diffusion of nutrients in the scaffold and diffusion of secreted molecules from the cells. Thus, the es-PLLA scaffold could represent a versatile tool also to generate mixed cell–scaffold devices, with potential application in many models of injury. RESCs cultured on this scaffold had a sustained proliferation, like BME-coated plastic, which is further increased by BME-conjugation, with a spontaneous tendency to grow stratified and to

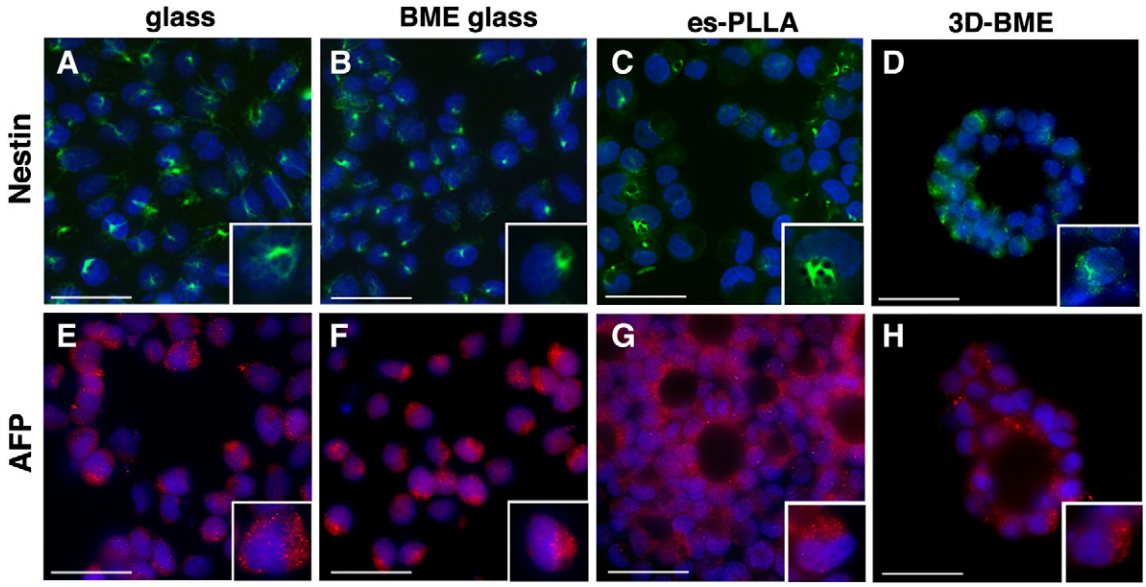

Fig. 4. Representative picture of differentiation markers after 7 DIV in different 2D and 3D culturing conditions. A–D: nestin (green) immunostained RESC cells; E–H: alpha-fetoprotein (AFP) immunostaining (red). Nuclei were counterstained with Hoechst33258 (blue). In each panel, the inset illustrates a high-power magnification of single cell, representative of marker's specific staining. 3D-culture induces cells to aggregate in follicle-like structures *Scale bar:* 20 μm. *Scale bar inset*: 12 μm.

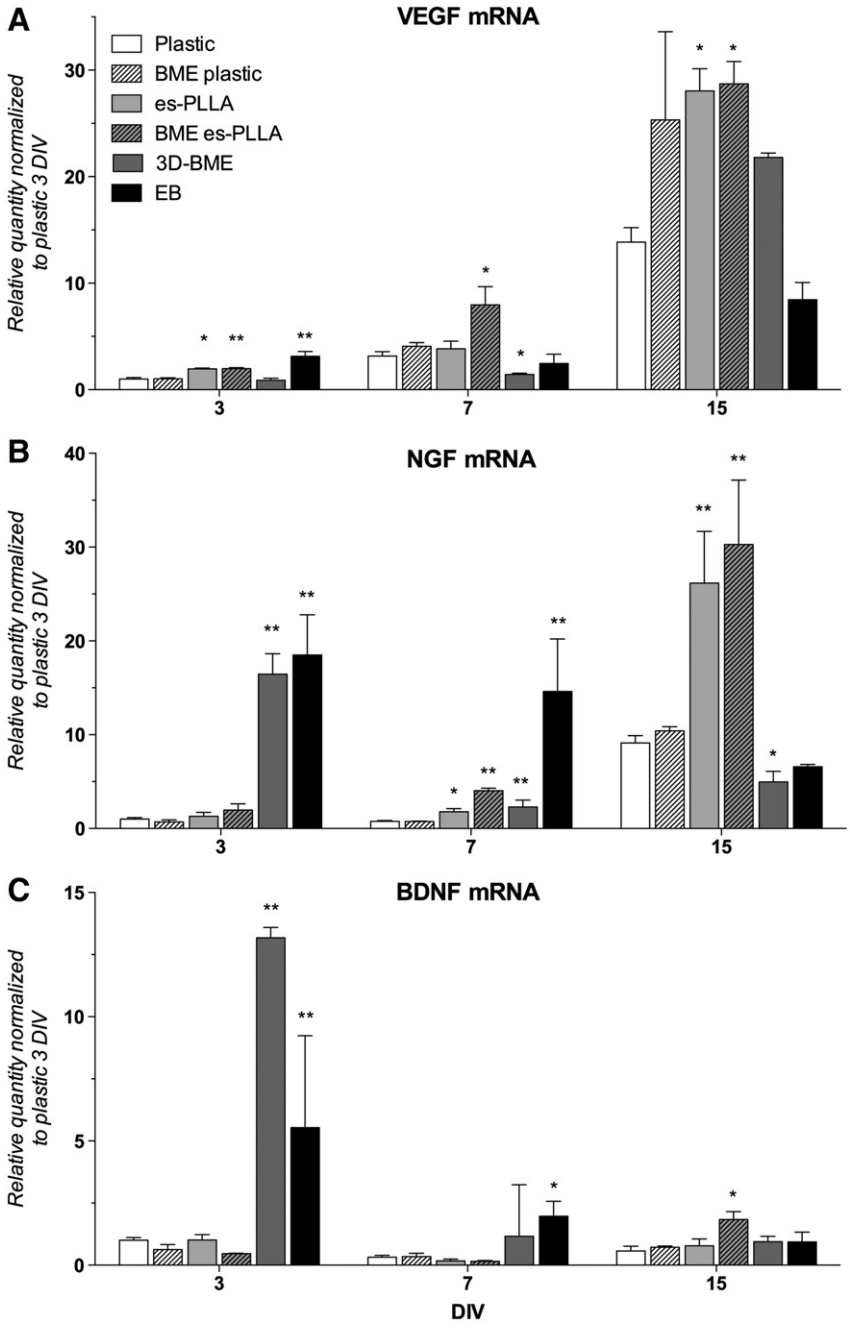

Fig. 5. Relative growth factors mRNA expression levels in RESCs grown in different culture conditions. Real-time PCR semiquantitative analysis of VEGF (A), NGF (B) and BDNF (C) mRNA expression in RESCs at 3, 7 and 15 DIV; relative expression levels were normalized *vs* plastic 3 DIV condition. *Statistical analysis:* two-way ANOVA was performed for mRNA expression analysis including culture conditions and time (discussed in the text). Each data set at 3, 7, 15 DIV was also analyzed by one-way ANOVA followed by Dunnett's *post-hoc* test using plastic as control. $^{*}p < 0.05$; $^{**}p < 0.01$.

organize into characteristic multi-layered, ring structures. Like the other tested cell/scaffold systems, the staining pattern of the three germ layers was stable and only a mild reduction in Oct4 mRNA was observed. According to our results and to our knowledge, the microenvironment created by electrospun nano- or microfibers is not sufficient *per se* to induce ES differentiation in the absence of other stimuli; however, topographic cues like fiber diameter and fiber alignment have been shown to influence proliferation of stem cells (Taqvi and Roy, 2006; Wang and Kisaalita, 2010; Feng et al., 2011; Wang et al., 2011).

We focused on the influence of 3D *vs* 2D chemical and mechanical properties on expression level of neuroprotective factors, like NGF, BDNF and VEGF. Different 2D and 3D culture conditions affect gene expression and growth factor production. 3D-BME scaffold promoted a sustained cellular production of BDNF and NGF in early culture. In long-term culture, es-PLLA electrospun scaffold either uncoated and BME coated, supported an intense VEGF and NGF mRNA synthesis followed by the release of biologically active proteins, as indicated by the bioactivity test on PC12 cells. Although a similar upregulation was observed also in plastic, es-PLLA scaffolds effectively improved this trend. These results could be related to cell–cell interaction and three-dimensional aggregate formation, since no differences were observed by providing exogenous ECM proteins (BME-coated surfaces).

Observed results could have implications for regenerative medicine applications. Recent studies suggest that secreted or released factors,

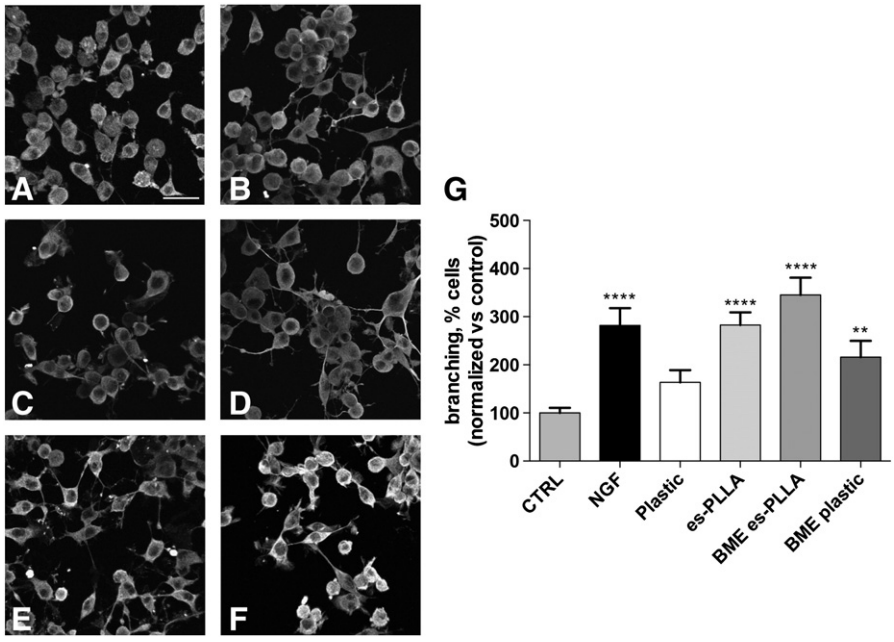

Fig. 6. *In vitro* test for NGF activity: neurite outgrowth in PC12 cells at 4 DIV. Panels A to C illustrate neurite elongation in PC12 cells visualized by β-III-Tubulin immunostaining in control conditions (A), in the presence of NGF 10 ng/ml (B) and in the presence of culture medium from RESC/plastic (C), RESC/es-PLLA culture (D), RESC/BME es-PLLA (E) and RESC/BME plastic culture(F). Scale bar: 30 μm. Graph in G illustrates the quantitative analysis, expressed as percentage of cells showing neuritis in the presence of NGF or RESC/es-PLLA conditioned media. Statistical analysis: one-way ANOVA and Dunnett's *post-hoc* test, $^{**}p < 0.01$; $^{****}p < 0.0001$.

rather than direct cell replacement, are responsible for most of the benefits observed after cell transplantation (Shimada and Spees, 2011), and in fact many attempts at growth factor controlled delivery using various implantable devices have been proposed (Straley et al., 2010; Lee et al., 2011). The introduction of mixed cell/scaffold devices could improve safety and efficacy of cell delivery and open new possibilities for the control of the fate of engrafted stem cells (Walker et al., 2009).

The culture conditions used in this study could be easily converted into implantable devices formed by scaffolds and cells. For example, 3D-BME embedded cells can be used to fill up cavities, like necrotic outcomes of ischemia and trauma (Chen et al., 2011). Moreover, due to good mechanical properties and high flexibility of es-PLLA, these scaffolds can be tailored to create sleeves to wrap nerves, or thin pocket filled of cell to be placed on the cerebral cortex surface, *etc.* (Walker et al., 2009; Han et al., 2010; Zurita et al., 2010; Jurga et al., 2011). Notably, RESCs grown on an es-PLLA scaffold had a higher production of bioactive NGF and VEGF than in standard 2D conditions, lasting for at least 2 weeks. Thus, a RESC/PLLA system able to restrain the cells inside the device, thus avoiding the migrations of cells into the tissue, but allowing paracrine communication, is attractive for the therapy of damaged peripheral nerve and neuropathic pain. This system could in fact represent a source of NGF and VEGF avoiding genetic manipulations and the diffusion of embryonic cells in the host, as already proposed for other tissues (Schneider et al., 2010; Sarkar et al., 2011). In fact, survival and regeneration of the peripheral sensory nerve require NGF and VEGF (Savignat et al., 2008; Ribeiro-Resende et al., 2009). Moreover, es-PLLA/RESC device could easily be removed after an appropriate time, thus avoiding possible side effects including pain (Pezet and McMahon, 2006; Tannemaat et al., 2008). Animal models of nerve injuries were challenged using acellular scaffolds releasing NT-3 (Johnson et al., 2009), GDNF (Moore et al., 2010), NGF (de Boer et al., 2010), or a combination of these factors (Madduri et al., 2010) to improve nerve regeneration. Thin-mesh sealed pocket might retain cells inside the scaffolds, to avoid embryonic cells dissemination in the host tissue, allowing in the meantime soluble molecules diffusion (*e.g.* NGF, VEGF). This mixed RESCs-PLLA device potentially couples the advantages of functionalized scaffolds and microenvironment-sensitive cells to improved NGF- and VEGF-sensitive tissue repair.

4. Experimental procedures

4.1. Maintenance of RESCs

Rat Embryonic Stem Cells (RESC clusters) were established from rat blastocyst and maintained as compact clusters on a murine embryonic fibroblast (MEF) feeder layer (Fernandez et al., 2011). All experiments were performed with a RESCs (RESC single cell) line. RESCs were obtained by cluster disruption and were routinely cultured as an adherent monolayer on standard cell culture plastics, without MEF, in DMEM/F12 (Gibco-Invitrogen, Milan, Italy), 10% Euromed embryonic stem cell quality fetal bovine serum (ES-FBS; Euroclone, Milan, Italy), 1× MEM/NEAA (Gibco-Invitrogen), 0.1 mM 2-Mercaptoethanol (Sigma, St. Louis, MO, USA), 3 mM nucleoside mix (Adenosine, Cytidine, Guanosine, Thymidine, Uridine; Sigma), 1× penicillin–streptomycin (Gibco-Invitrogen). RESCs were maintained at 37 °C in a humidified 5% CO_2, 95% air atmosphere incubator, and were sub-cultured at confluence, approximately once every 3–4 days. Cells were first washed with PBS (Gibco-Invitrogen) and then incubated with 0.05% trypsin (Trypsin-EDTA, Gibco-Invitrogen) for 2 min at 37 °C. After stopping trypsinization with ES-FBS, cells were centrifuged at 400 ×*g* for 5 min; the pellet was re-suspended in standard culture media and counted with a Scepter cell counter (Millipore, Billerica, MA, USA). Cells were finally plated at a density of 5–10 × 10^3 cells/cm^2.

For immunofluorescent analysis RESCs were seeded on glass coverslips at a density of 1–10 × 10^3 cells/cm^2 and cultured in the same standard media for 3–15 DIV.

4.2. Cell culture substrates

Poly-(L-lactic acid) (PLLA, Lacea H.100-E, Mitsui Fine Chemicals, Germany; $M_w = 8.4 \times 10^4$ g/mol, PDI = 1.7) scaffolds (es-PLLA) were fabricated by electrospinning from a solution of 13% w/v PLLA in dichloromethane (DCM, Sigma-Aldrich) and dimethylformamide

(DMF, Sigma-Aldrich) volume ratio 65:35), under the following conditions: applied voltage = 12 kV, needle to collector distance = 15 cm, solution flow rate = 15×10^{-3} ml/min, at room temperature (RT) and relative humidity RH = 40–50%. Electrospun mats were kept under vacuum over P_2O_5 at RT overnight in order to remove residual solvents. Highly porous mats with micro-scale interstitial pores and a random orientation of the sub-micrometric fibers were obtained (mean diameter distribution: 620 ± 150 nm) (Fig. 1A). Scaffolds were cut into suitably sized pieces and assembled with CellCrown™ support (Scaffdex, Tampere, Finland). Scaffold sterilization was carried out as follows: washing 1 h in EtOH 90%, then hydrating in EtOH 70% for 30 min. Ethanol was removed by washing twice in PBS for 10 min, then 2 × 10 min in DMEM/F12 supplemented with 2% (v/v) (Gibco-Invitrogen). Es-PLLA scaffolds were assembled in a 24-well plate and incubated overnight in DMEM/F12 with antibiotics, under UV light. They were rinsed three times with PBS before cell seeding.

Cultrex® Basement Membrane Extract (BME) (Trevigen®, Gaithersburg, MD, USA) was used to coat plastic/glass substrates (BME plastic/glass) and electrospun PLLA scaffolds (BME es-PLLA). In order to obtain a non-gelling coating solution, Cultrex® BME was thawed on ice and diluted in DMEM/F12 (final concentration 0.5 mg/ml). The plastic/glass or the PLLA scaffolds were covered with the diluted Cultrex® BME and incubated overnight at 37 °C. The coating solution was removed just before cell seeding.

3D-Culture Matrix™ Basement Membrane Extract (Trevigen®) was used in the form of gel with cells entrapped as a three-dimensional growth substrate (3D-BME).

4.3. Culture of RESCs on different substrates

4.3.1. Es-PLLA scaffolds

RESCs were harvested as previously described, re-suspended in standard RESCs medium then plated upon es-PLLA scaffolds (in 24-well plate) at a cell density of 1–10 × 10^3 cells/cm^2. The culture was maintained in standard RESCs medium for 3–15 DIV and the medium was replaced every 2–3 days or more frequently, if necessary.

4.3.2. BME-coated surfaces

Cells were seeded at a density of 1–5 × 10^3 cells/cm^2 and maintained in standard RESCs medium for 3–15 DIV.

4.3.3. Cell encapsulation in 3D-Culture Matrix™ BME (3D-BME)

Sub-confluent RESCs were harvested, re-suspended in a small volume of DMEM/F12 and mixed with ice-cold 3D-Culture Matrix™ BME. The final suspension had a cell density of 9–14 × 10^3 cells/100 μl and contained 95% (v/v) 3D-Culture Matrix™ BME, 5% (v/v) cell suspension in DMEM/F12. A suitable volume of RESCs/3D-Culture Matrix™ BME suspension was gently plated on (a) glass coverslips for immunohistochemistry processing and RT-PCR analysis, (b) a 96-well plate for MTT assay. All these procedures were performed quickly with ice-cold materials to prevent early gelling. Once plated, the 3D-BME suspension was incubated for at least 30 min at 37 °C in a humidified atmosphere to allow gel transition. 3D cell-entrapped gels were cultured in standard RESCs medium supplemented with dissolved 3D-Culture Matrix™ BME (final concentration 2% v/v). The culture was maintained for 3–15 DIV and the medium was replaced every 2–3 days, or more frequently if necessary.

In order to induce *embryoid body* (*EB*) formation, a "hanging drop" method was followed. Briefly, RESCs were harvested by trypsinization, centrifuged 5 min 400 ×*g*, re-suspended in standard RESCs medium and counted. A cell suspension of 2 × 10^4 cells/ml in RESCs medium supplemented with 10 ng/ml bFGF (Euroclone) was prepared. Drops of 20 μl containing 400 cells were distributed on the inner side of a lid of a non culture-treated dish (Corning, NY, USA), while the bottom was filled with 10 ml PBS to create ideal humidity. After 2 days incubation (37 °C, 5% CO_2), drops containing cell aggregates were transferred to a non culture-treated 4-well plate (Nunc, Denmark) with fresh RESCs medium supplemented with 10 ng/ml bFGF. EB were cultured for 2–4 days before changing the medium. In order to replace the medium, the EB suspension was collected in a tube and allowed to settle for 20 min; the medium was then removed and a fresh one carefully added. Finally, the EB suspension was transferred to a 6-well ultra-low attachment culture plate (Corning), and maintained for 6–10 days with regular medium changes every 3 days.

4.4. MTT assay

Viability and proliferation of RESCs cultured on the different substrates were assessed using MTT assay. Tests were performed at three time points (1, 3, 5 DIV) in three independent experiments, each performed in duplicate. Cells were seeded at the density of 12,500 cells/cm^2 in (a) a 96-well plate, on plastic cell-culture treated, BME plastic, and 3D-BME, (b) a 24-well plate for es-PLLA scaffolds. At each time point, cells were incubated in 0.5 mg/ml MTT (Sigma) dissolved in Opti-MEM (Gibco-Invitrogen) for 3 h at 37 °C. In order to dissolve formazan crystals, a solubilization solution containing 80% Isopropanol (IBI Scientific, Peosta, IA, USA), 10% Triton-X 100, 10% HCl 0.1 N (Sigma) was added and incubated for 1 h under gentle shaking at room temperature. Absorbance was measured at 570 nm using the Microplate Reader Model 680 (BioRad, Milan, Italy). Final results were calculated from the mean of replicates and standardized on the absorbance at 1 DIV.

4.5. Immunocytochemistry

Indirect immunofluorescence (IF) procedures were used to study RESCs cultured on glass coverslips, es-PLLA scaffolds and BME coated surfaces. Cells were washed in PBS and fixed in 4% paraformaldehyde in 0.1 M Sørensen phosphate buffer for 20 min at RT. Subsequently, fixed cells were blocked in PBS containing 0.3% Triton-X 100 (Merck, Darmstadt, Germany), 5% Donkey Normal Serum (Sigma) for 1 h at RT, then incubated overnight at 4 °C in humid atmosphere with primary antibodies diluted in blocking solution. After rinsing in PBS (2 × 10 min), cells were incubated with fluorochrome-labeled secondary antisera diluted in PBS, 0.3% Triton-X 100 for 30 min at 37 °C. The primary and secondary antibodies are listed in Tables 1 and 2, respectively. For nuclear staining, cells were first washed in PBS then incubated 15 min in PBS containing 1 μg/ml Hoechst 33258, 0.2% Triton-X 100. After rinsing in PBS, cells were finally mounted in glycerol containing 0.1% 1,4-phenylendiamine (Sigma). Negative controls were performed by primary antibody omission.

In order to perform immunohistochemical staining of 3D-BME, cell-entrapped gels were fixed in 4% paraformaldehyde in 0.1 M Sørensen phosphate buffer for 2.5 h, then rinsed in PBS (2 × 15 min). Gels were cryoprotected in 5% sucrose, frozen by CO_2 and sectioned using a cryostat (Microm HM 550, Thermo Fisher Scientific, Waltham, MA, USA).

Table 1
Primary antibodies used in the study for the immunocytochemistry reactions.

Antibody	Antigen	Species	Supplier	Dilution
Actin	C-terminus peptide of Actin of human origin	Goat	Santa Cruz	1:150
AFP	C-terminus peptide of alpha fetoprotein of human origin	Goat	Santa Cruz	1:50
Caspase3	Active human pro-caspase3 fragment	Rabbit	Pharmingen	1:150
Nestin	Rat nestin	Mouse	Pharmingen	1:500
Oct4	Synthetic peptide conjugated to KLH derived from within residues 300 to C-terminus of human Oct4	Rabbit	AbCam	1:50
β-III-Tubulin	Microtubules derived from rat brain	Mouse	R&D systems	1:1000

Table 2
Secondary antibodies used in the study for the immunocytochemistry reactions.

Secondary antibody	Species	Supplier	Dilution
RRX-anti mouse	Donkey	Jackson	1:100
Cy2-anti mouse	Donkey	Jackson	1:100
RRX-anti rabbit	Donkey	Jackson	1:100
Cy2-anti rabbit	Donkey	Jackson	1:100
RRX-anti goat	Donkey	Jackson	1:100
Alexa488-anti goat	Donkey	Molecular Probes-Invitrogen	1:600

Sections (14 μm thick) were collected on gelatin-coated slides, incubated in 0.1 M PBS at RT for 10–30 min and subjected to the immunofluorescence procedure described above.

4.6. RNA isolation, retrotranscription and semi-quantitative real time PCR

Total RNA from RESCs cultured on each substrate was extracted following the manufacturer's specifications (Micro RNeasy kit, Qiagen, Milan Italy). After DNase treatment (1 U/μl, 1× DNase buffer, 2 U/μl ribonuclease inhibitor, at 37 °C for 30 min) (Fermentas, Life Sciences, Italy), RNAs were retrotranscribed using the enzyme M-Moloney murine leukemia virus reverse transcriptase (M-MuLV-RT, 10 U/μl) (Fermentas), in the presence of 1× first strand buffer, 1 mM d(NTP)s (Fermentas), 25 ng/μl oligo $d(T)_{18}$ (Fermentas), incubating at 42 °C for 60 min. The cDNAs obtained were processed for real-time PCR using the Mx3005P QPCR System (Stratagene, La Jolla, CA, USA) equipped with an FAM™/SYBR® Green I filter (492 nm excitation–516 nm emission). SYBR Green I fluorescent detection was the real-time PCR chemistry chosen to perform these experiments. PCR was performed in a final volume of 25 μl and the reaction mix was composed of cDNA, 1× Maxima™ SYBR Green/ROX qPCR Master Mix (Fermentas) and 0.4 μM of each primer (sense and antisense). The sequences of primers employed are shown in Table 3. PCR started with 1 cycle at 95 °C for 10 min, followed by specific conditions for each primer as shown in Table 3; at the end of the amplification cycles the dissociation curve was performed by following a procedure consisting of first incubating sample at 95 °C for 1 min to denature the PCR-amplified products, then ramping temperature down to 55 °C and finally increasing temperature from 55 °C to 95 °C at the rate of 0.2 °C/s, continuously collecting over the temperature ramp. The specificity of the amplified product was controlled by the presence of one peak at the expected melting temperature. Random amplified products were resolved by electrophoresis in 2.5% agarose gel stained with ethidium bromide, in order to check the specificity of the PCR reaction. This was confirmed by the presence of a single band of the expected size. A 100 bp DNA ladder (Fermentas) was used as DNA marker.

Table 3
Primers and conditions used for real time semiquantitative PCR reactions. All primers were obtained from MWG Operon (Ebersberg, Germany), except Oct4, obtained from IDT (Coralville, IA, USA).

Gene	Acc. no.	Sequences (x–y)	Conditions
GAPDH	M17701	5-GGCAAGTTCAATGGCACAGTCAAG-3 5-ACATACTCAGCACCAGCATCACC-3	95 °C 30 s 60 °C 60 s 40 cycles
Oct4	NM_001009178	5-GCCTTTCCCTCTGTTCCTGT-3 5-GTCTACCTCCCTTCCTTGCC-3	95 °C 30 s 60 °C 60 s 40 cycles
VEGF	NM_031836	5-ATATCTTCAAGCCGTCCTG-3 5-TTCTATCTTTCTTTGGTCTGC-3	95 °C 30 s 60 °C 60 s 40 cycles
NGF	M36589	5-GACGACTCTTCTCTTCCAG-3 5-CGTGGCTGTGGTCTTATCTC-3	95 °C 30 s 60 °C 45 s 40 cycles
BDNF	NM_012513	5-GTGACAGTATTAGCGAGTGG-3 5-GCCTTCCTTCGTGTAACC-3	95 °C 30 s 60 °C 45 s 40 cycles

Semi-quantitative analysis was performed on the values of the threshold cycle (Ct) obtained for each sample, with GAPDH as housekeeping gene. The relative gene expression was calculated using the formula $2^{(-\Delta\Delta Ct)}$ and a defined group as reference ($2^{(-\Delta\Delta Ct)} = 1$).

4.7. Microscopy and image analysis

Cells were observed and photographed by a Nikon Eclipse E600 fluorescence microscope (Nikon, Italy) equipped with digital CCD camera Q Imaging Retiga-2000RV (Q Imaging, Surrey, BC, Canada) using a 40× objective. To capture images and quantitative analysis NIS Elements (Nikon) software was used. The system is capable of serially producing optical sectioning (0.5 μm) throughout fluorescent specimens with a thickness range of up to 600 μm. The cross-sectional image series of a thick specimen is collected by coordinating incremental changes in the microscope fine focus mechanism (using a stepper motor) with sequential image acquisition, in a step-by-step manner. The deconvoluted 2D image slices were reconstructed into a composite 3D image of the required thickness. Samples were also analyzed by confocal laser microscopy (Nikon A1R) to generate serial optic sectioning of 3D specimens.

The percentage of Caspase3 was assessed by counting the number of immunoreactive cells (out of the total nuclei) in at least five fields for each sample, to obtain a minimum number of 100 cells/sample. For the analysis of pyknotic nuclei, the percentage of pyknotic and fragmented nuclei on total number of cells for each substrate was considered.

4.8. PC12 cell culture and neuritis elongation test

Rat pheochromocytoma cell line 12 (PC12) (ATCC-Italy) was cultured in DMEM (Gibco-invitrogen) supplemented with 10% horse serum (Gibco-invitrogen), 5% FBS (Gibco-invitrogen), 2 mM glutamine, 100 U/ml penicillin, and 100 g/ml streptomycin at 37 °C in a 5% CO_2 incubator. In order to study neuritis elongation, cells were seeded at 5×10^3 cells/well on 24 multi-well plates with 12 mm cover glass coated with poly-L-Lysine (PLL) (Sigma). 24 h after seeding, cells were treated 1:1 conditioned medium/DMEM supplemented with 0.5% FBS 1% horse serum with medium derived from: RESCs/plastic (12 DIV), RESCs/es-PLLA (15 DIV), RESCs/BME es-PLLA(12 DIV) and RESCs/BME plastic (13 DIV) culture systems. Positive control (NGF) was treated with NGF (10 ng/ml; a generous gift from Dr. L. Aloe, Inst. Neurobiol. Mol. Med., CNR, Rome, Italy) in DMEM supplemented with 0.5% FBS 1% horse serum. Medium was changed every 2 days.

After 4 days of treatment, cells were fixed in 4% paraformaldehyde and processed for β-III-Tubulin IF-staining. In order to perform branching analysis, 5 images per glass (8 glasses for each treatment) were taken with a 40× objective. Only cells whose neuritis length was found to be equal or longer than the diameter of the cell body were considered for cell counting.

Acknowledgments

This work has been supported by POR-FESR, progetto Tecnopoli (LC, MLF), Regione Emilia Romagna, and by Montecatone Rehabilitation Institute, Imola (LC).

References

Blancas, A.A., Chen, C.S., Stolberg, S., McCloskey, K.E., 2011. Adhesive forces in embryonic stem cell cultures. Cell Adh. Migr. 5, 472–479.
Brizzi, M.F., Tarone, G., Defilippi, P., 2012. Extracellular matrix, integrins, and growth factors as tailors of the stem cell niche. Curr. Opin. Cell Biol. 24, 645–651.
Chen, S.S., Fitzgerald, W., Zimmerberg, J., Kleinman, H.K., Margolis, L., 2007. Cell–cell and cell–extracellular matrix interactions regulate embryonic stem cell differentiation. Stem Cells 25, 553–561.

Chen, J., Ye, X., Yan, T., Zhang, C., Yang, X.P., Cui, X., Cui, Y., Zacharek, A., Roberts, C., Liu, X., Dai, X., Lu, M., Chopp, M., 2011. Adverse effects of bone marrow stromal cell treatment of stroke in diabetic rats. Stroke 42, 3551–3558.

de Boer, R., Knight, A.M., Spinner, R.J., Malessy, M.J., Yaszemski, M.J., Windebank, A.J., 2010. *In vitro* and *in vivo* release of nerve growth factor from biodegradable poly-lactic-co-glycolic-acid microspheres. J. Biomed. Mater. Res. 95, 1067–1073.

Dickinson, L.E., Kusuma, S., Gerecht, S., 2011. Reconstructing the differentiation niche of embryonic stem cells using biomaterials. Macromol. Biosci. 11, 36–49.

Edalat, F., Bae, H., Manoucheri, S., Cha, J.M., Khademhosseini, A., 2012. Engineering approaches toward deconstructing and controlling the stem cell environment. Ann. Biomed. Eng. 40, 1301–1315.

Feng, G., Jin, X., Hu, J., Ma, H., Gupte, M.J., Liu, H., Ma, P.X., 2011. Effects of hypoxias and scaffold architecture on rabbit mesenchymal stem cell differentiation towards a nucleus pulposus-like phenotype. Biomaterials 32, 8182–8189.

Fernandez, M., Pirondi, S., Chen, B.L., Del Vecchio, G., Alessandri, M., Farnedi, A., Pession, A., Feki, A., Jaconi, M.E., Calzà, L., 2011. Isolation of rat embryonic stem-like cells: a tool for stem cell research and drug discovery. Dev. Dyn. 240, 2482–2494.

Gerlach, J.C., Hout, M., Edsbagge, J., Bjorquist, P., Lubberstedt, M., Miki, T., Stachelscheid, H., Schmelzer, E., Schatten, G., Zeilinger, K., 2010. Dynamic 3D culture promotes spontaneous embryonic stem cell differentiation *in vitro*. Tissue Eng. Part C Methods 16, 115–121.

Han, Q., Jin, W., Xiao, Z., Ni, H., Wang, J., Kong, J., Wu, J., Liang, W., Chen, L., Zhao, Y., Chen, B., Dai, J., 2010. The promotion of neural regeneration in an extreme rat spinal cord injury model using a collagen scaffold containing a collagen binding neuroprotective protein and an EGFR neutralizing antibody. Biomaterials 31, 9212–9220.

Heydarkhan-Hagvall, S., Gluck, J.M., Delman, C., Jung, M., Ehsani, N., Full, S., Shemin, R.J., 2012. The effect of vitronectin on the differentiation of embryonic stem cells in a 3D culture system. Biomaterials 33, 2032–2040.

Johnson, C.E., Crawford, B.E., Stavridis, M., Ten Dam, G., Wat, A.L., Rushton, G., Ward, C.M., Wilson, V., van Kuppevelt, T.H., Esko, J.D., Smith, A., Gallagher, J.T., Merry, C.L., 2007. Essential alterations of heparan sulfate during the differentiation of embryonic stem cells to Sox1-enhanced green fluorescent protein-expressing neural progenitor cells. Stem Cells 25, 1913–1923.

Johnson, P.J., Parker, S.R., Sakiyama-Elbert, S.E., 2009. Controlled release of neurotrophin-3 from fibrin-based tissue engineering scaffolds enhances neural fiber sprouting following subacute spinal cord injiury. Biotechnol. Bioeng. 104, 1207–1214.

Johnson, P.J., Tatara, A., Shiu, A., Sakiyama-Elbert, S.E., 2010. Controlled release of neurotrophin-3 and platelet derived growth factor from fibrin scaffolds containing neural progenitor cells enhances survival and differentiation into neurons in a subacute model of SCI. Cell Transplant. 19, 89–101.

Jurga, M., Dainiak, M.B., Sarnowska, A., Jablonska, A., Tripathi, A., Plieva, F.M., Savina, I.N., Strojek, L., Jungvid, H., Kumar, A., Lukomska, B., Domanska-Janik, K., Forraz, N., McGuckin, C.P., 2011. The performance of laminin-containing cryogel scaffolds in neural tissue regeneration. Biomaterials 32, 3423–3434.

Kraushaar, D.C., Dalton, S., Wang, L., 2013. Heparan sulfate: a key regulator of embryonic stem cell fate. Biol. Chem. 394, 741–751.

Lee, K., Silva, E.A., Mooney, D.J., 2011. Growth factor delivery-based tissue engineering: general approaches and a review of recent developments. J. R. Soc. Interface 8, 153–170.

Levenmberg, S., Huang, N.F., Lavik, E., Rogers, A.B., Itskovitz-Eldor, J., Langer, R., 2003. Differentiation of human embryonic stem cells on three-dimensional polymer scaffolds. Proc. Natl. Acad. Sci. U. S. A. 100, 12741–12746.

Li, Z., Leung, M., Hopper, R., Ellenbogen, R., Zhang, M., 2010. Feeder-free self-renewal of human embryonic stem cells in 3D porous natural polymer scaffolds. Biomaterials 31, 404–412.

Madduri, S., di Summa, P., Papaloizos, M., Kalbermatten, D., Gander, B., 2010. Effect of controlled co-delivery of synergistic neurotrophic factors on early nerve regeneration in rats. Biomaterials 31, 8402–8409.

Moore, A.M., Wood, M.D., Chenard, K., Hunter, D.A., Mackinnon, S.E., Sakiyama-Elbert, S.E., Borschel, G.H., 2010. Controlled delivery of glial cell line-derived neurotrophic factor enhances motor nerve regeneration. J. Hand Surg. Am. 35, 2008–2017.

Ou, D.B., He, Y., Chen, R., Teng, J.W., Wang, H.T., Zeng, D., Liu, X.T., Ding, L., Huang, J.Y., Zheng, Q.S., 2011. Three-dimensional co-culture facilitates the differentiation of embryonic stem cells into mature cardiomyocytes. J. Cell. Biochem. 112, 3555–3562.

Pezet, S., McMahon, S.B., 2006. Neurotrophins: mediators and modulators of pain. Annu. Rev. Neurosci. 29, 507–538.

Pineda, E.T., Nerem, R.M., Ahsan, T., 2013. Differentiation patterns of embryonic stem cells in two- versus three-dimensional culture. Cells Tissues Organs 197, 399–410.

Ribeiro-Resende, V.T., Pimentel-Coelho, P.M., Mesentier-Louro, L.A., Mendez, R.M.B., Mello-Silva, J.P.C., Cabral-da-Silva, M.C., 2009. Trophic activity derived from bone marrow mononuclear cells increases peripheral nerve regeneration by acting on both neuronal and glial cell populations. Neuroscience 159, 540–549.

Sarkar, D., Ankrum, J.A., Teo, G.S., Carman, C.V., Karp, J.M., 2011. Cellular and extracellular programming of cell fate through engineered intracrine-, paracrine-, and endocrine-like mechanisms. Biomaterials 32, 3053–3061.

Savignat, M., Vodoube, C., Ackermann, A., Haikel, Y., 2008. Evaluation of early nerve regeneration using a polymeric membrane functionalized with nerve growth factor (NGF) after a crush lesion of the rat mental nerve. J. Oral Maxillofac. Surg. 66, 711–717.

Schenke-Layland, K., Angelis, E., Rhodes, K.E., Heydarkhan-Hagvall, S., Mikkola, H.K., Maclellan, W.R., 2007. Collagen IV induces trophoectoderm differentiation of mouse embryonic stem cells. Stem Cells 25, 1529–1538.

Schneider, R.K., Anraths, J., Kramann, R., Bornemann, J., Bovi, M., Knüchel, R., Neuss, S., 2010. The role of biomaterials in the direction of mesenchymal stem cell properties and extracellular matrix remodelling in dermal tissue engineering. Biomaterials 31, 7948–7959.

Shimada, I.S., Spees, J.L., 2011. Stem and progenitor cells for neurological repair: minor issues, major hurdles, and exciting opportunities for paracrine-based therapeutics. J. Cell. Biochem. 112, 374–380.

Straley, K.S., Wong Po Foo, C., Heilshorn, S.C., 2010. Biomaterial design strategies for the treatment of spinal cord injuries. J. Neurotrauma 27, 1–19.

Tamm, C., Kjellén, L., Li, J.P., 2012. Heparan sulfate biosynthesis enzymes in embryonic stem cell biology. J. Histochem. Cytochem. 60, 943–949.

Tannemaat, M.R., Eggers, R., Hendriks, W.T., de Ruiter, G.C.W., van Heerikhuize, J.J., Pool, C.W., Malessy, M.J., Boer, G.J., Verhaagen, J., 2008. Differential effects of lentiviral vector-mediated overexpression of nerve growth factor and glial cell line-derived neurotrophic factor on regenerating sensory and motor axons in the transected peripheral nerve. Eur. J. Neurosci. 28, 1467–1479.

Taqvi, S., Roy, K., 2006. Influence of scaffold physical properties and stromal cell coculture on hematopoietic differentiation of mouse embryonic stem cells. Biomaterials 27, 6024–6031.

Uemura, M., Refaat, M.M., Shinoyama, M., Hayashi, H., Hashimoto, N., Takahashi, J., 2010. Matrigel supports survival and neuronal differentiation of grafted embryonic stem cell-derived neural precursor cells. J. Neurosci. Res. 88, 542–551.

Walker, P.A., Aroom, K.R., Jimenez, F., Shah, S.K., Harting, M.T., Gill, B.S., Cox Jr., C.S., 2009. Advances in progenitor cell therapy using scaffolding constructs for central nervous system injury. Stem Cell Rev. 5, 283–300.

Wang, L., Kisaalita, W.S., 2010. Characterization of micropatterned nanofibrous scaffolds for neural network activity readout for high-throughput screening. J. Biomed. Mater. Res. B Appl. Biomater. 94, 238–249.

Wang, J., Ma, H., Jin, X., Hu, J., Liu, X., Ni, L., Ma, P.X., 2011. The effect of scaffold architecture on odontogenic differentiation of human dental pulp stem cells. Biomaterials 32, 7822–7830.

Xie, J., Willerth, S.M., Li, X., Macewan, M.R., Rader, A., Sakiyama-Elbert, S.E., Xia, Y., 2009. The differentiation of embryonic stem cells seeded on electrospun nanofibers into neural lineages. Biomaterials 30, 354–362.

Yang, F., Murugan, R., Wang, S., Ramakrishna, S., 2004. Electrospinning of nano/micro scale poly(L-lactic acid) aligned fibers and their potential in neural tissue engineering. Biomaterials 26, 2603–2610.

Zapata, A.G., Alfaro, D., García-Ceca, J., 2012. Biology of stem cells: the role of microenvironments. Adv. Exp. Med. Biol. 741, 135–151.

Zhang, Y.H., Zhao, C.Q., Jiang, L.S., Dai, L.Y., 2011. Substrate stiffness regulates apoptosis and the mRNA expression of extracellular matrix regulatory genes in the rat annular cells. Matrix Biol. 30, 135–144.

Zurita, M., Otero, L., Aguayo, C., Bonilla, C., Ferreira, E., Parajón, A., Vaquero, J., 2010. Cell therapy for spinal cord repair: optimization of biologic scaffolds for survival and neural differentiation of human bone marrow stromal cells. Cytotherapy 12, 522–537.